Available online at www.sciencedirect.com
SCIENCE DIRECT
Journal of Photochemistry and Photobiology A: Chemistry 180 (2006) 289–299
Journal of Photochemistry and Photobiology A:Chemistry
www.elsevier.com/locate/jphotochem

Selective excitation of molecular modes in a mixture by optimal control of electronically nonresonant femtosecond four-wave mixing spectroscopy

J. Konradi, A.K. Singh, A. Materny *

International University Bremen, School of Engineering and Science, Campus Ring 1, D-28759 Bremen, Germany

Available online 10 March 2006

Abstract

Femtosecond time-resolved coherent anti-Stokes Raman scattering (fs-CARS) gives access to ultrafast molecular dynamics. Due to the spectrally broad laser pulses, usually poorly resolved spectra result from this spectroscopy. However, it can be demonstrated that by shaping the femtosecond pulses a selective excitation of specific vibrational modes is possible. We demonstrate that using a feedback-controlled optimization technique, molecule-specific CARS spectra can be obtained from a mixture of different substances. A careful analysis of the experimental results points to a nontrivial control of the vibrational mode dynamics in the electronic ground state of the molecules as underlying mechanism.

Keywords: Femtosecond spectroscopy; Optimal control; Nonlinear four-wave mixing spectroscopy; Mixtures; Raman spectroscopy

1. Introduction

The availability of commercial femtosecond laser systems makes the development of new techniques and applications of time-domain spectroscopy even more attractive. Many research groups use the ultrashort pulses in order to learn more about molecular and reaction dynamics even in complex biological systems. Since the high powers of femtosecond laser pulses favor nonlinear optical processes, also higher order nonlinear spectroscopy like coherent anti-Stokes Raman scattering (CARS) results in intense signals. In principle, an application of femtosecond light sources would also be of interest for enhancing the nonlinear signal in experiments, where spectral resolution is demanded. Unfortunately, the use of femtosecond lasers limits the spectral resolution considerably due to the inherently broad spectral bandwidth [1,2]. Several modes falling within the broad spectrum of femtosecond pulses are coherently excited [3,4].

The use of femtosecond laser pulses allows for an interaction with molecules on the time-scale of elementary chemical processes like bond breaking and formation. Therefore, a mode-specific excitation appears to be the key to selective chemistry. Already in the early time of femtosecond spectroscopy, coherent control techniques were applied in order to drive molecular dynamics into the desired direction [5–7]. The induced dynamics strongly depend on the electric field properties of the exciting laser pulses. A prediction of the pulse shape required for a mode control in complex molecular systems, which also takes into account experimental particularities, is at least very demanding. A solution to apply control also to more complicated molecules has been suggested by Judson and Rabitz [8]. Here, the pulse shaper setup is controlled by an evolutionary algorithm, which uses the signal arising from the laser–molecule interaction as fitness function for the optimization [9]. This self-learning loop approach has been successfully used by several groups for the control of chemical processes [10–13].

Recently, we have performed femtosecond time-resolved CARS experiments on polymers of different diacetylenes. There, we could demonstrate that only slight changes of the chirp of the stimulated Raman pump or Stokes laser pulses resulted in dramatically changed fs-CARS spectra and transients [4]. Applying the feedback control technique, the selective excitation of specific vibrational modes resulted in a nearly complete suppression of the other mode contributions in the nonlinear Raman spectra [14]. Interestingly, the focussing of the energy into one mode persisted over the full coherence lifetime of the transient. In these experiments, the exciting laser pulses were in resonance with the polymer absorption. It is well known, that in the excited excitonic state of the polydiacetylenes, fast dynamics take place.

* Corresponding author. Tel.: +49 421 2003231.
E-mail address: a.materny@iu-bremen.de (A. Materny).

1010-6030/$ – see front matter © 2006 Elsevier B.V. All rights reserved.
doi:10.1016/j.jphotochem.2006.02.009

Therefore, the change of this excited state dynamics played a key role in the explanation of the control mechanism [15,16]. Without doubt, the dynamics in the excited state has to be taken into account, when shaped laser pulses interact resonantly with a molecular system. Nevertheless, ground state dynamics could also be involved. In order to investigate this closer, we have conducted CARS experiments on different molecular systems under electronically nonresonant excitation conditions [17]. In the following, we will present results obtained from a liquid mixture of benzene and chloroform. We will demonstrate that the self-learning loop approach also involves nontrivial mechanisms, which rely on molecule-specific mode control in the electronic ground state of the different molecular species.

2. Theory

In our experiments, coherent anti-Stokes Raman scattering (CARS) is observed from molecules, which have no absorption in the visible spectral range. This nonresonant interaction with the quantum system can be described by established theoretical models [18]. In the model introduced in the following [19,20], the CARS signal induced by a nonlinear interaction of the pump pulse $\tilde{\varepsilon}_{\mathrm{p}}$, Stokes pulse $\tilde{\varepsilon}_{\mathrm{S}}$, and probe pulse $\tilde{\varepsilon}_{\mathrm{pr}}$ in the sample with the intermediate levels $|m\rangle$, $|n\rangle$, $|l\rangle$, and the ground state $|g\rangle$ is described by the third-order polarization in the time-domain:

$$p^{(3)}(t) \propto -\frac{1}{\hbar^3}\sum_{mnl}\mu_{gl}\mu_{ln}\mu_{mn}\mu_{mg}\, exp[-(\mathrm{i}\omega_{lg}+\Gamma_{lg})t] \times \int_{-\infty}^{t}\mathrm{d}t_1\int_{-\infty}^{t_1}\mathrm{d}t_2\int_{-\infty}^{t_2}\mathrm{d}t_3\tilde{\varepsilon}_{\mathrm{p}}(t_3)\tilde{\varepsilon}_{\mathrm{s}}^{*}(t_2)\tilde{\varepsilon}_{\mathrm{pr}}(t_1)\ \exp[(\mathrm{i}\omega_{ln} +\Gamma_{ln})t_1]\ \exp[(-\mathrm{i}\omega_{mn}+\Gamma_{mn})t_2]\ \exp[(\mathrm{i}\omega_{mg}+\Gamma_{mg})t_3], \quad (1)$$

where μ_{ij} are the dipole moments of the transitions with the frequencies $\omega_{ij} = (E_i - E_j)/\hbar$. If all intermediate states are far from resonance, the third-order polarization of the nonresonant transitions is approximated in the frequency domain by

$$P_{\mathrm{nr}}^{(3)}(\omega) \propto \int_0^{\infty}\mathrm{d}\Omega\varepsilon_{\mathrm{pr}}(\omega-\Omega)\int_0^{\infty}\mathrm{d}\omega_1\varepsilon_{\mathrm{s}}^{*}(\omega_1-\Omega)\varepsilon_{\mathrm{p}}(\omega). \quad (2)$$

For a singly resonant Raman transition via the intermediate level $|i\rangle$ the nonlinear polarization is given by the expression:

$$P_{\mathrm{r}}^{(3)}(\omega) \propto \int_0^{\infty}\mathrm{d}\Omega\frac{\varepsilon_{\mathrm{pr}}(\omega-\Omega)}{(\omega_{\mathrm{R}}-\Omega)+i\Gamma}\int_0^{\infty}\mathrm{d}\omega_1\varepsilon_{\mathrm{s}}^{*}(\omega_1-\Omega)\varepsilon_{\mathrm{p}}(\omega_1), \quad (3)$$

where ω_{R} is the resonance frequency and Γ is the bandwidth of the Raman level. In both cases, the integral term of the complex pulse amplitudes describes the second-order polarization responsible for the excitation of the molecular vibrations. The excitation amplitude of the Raman mode induced by the nonlinear interaction of pump and Stokes pulses having a frequency difference of Ω is

$$A(\Omega) = \int_0^{\infty}\mathrm{d}\omega_1\varepsilon_{\mathrm{s}}^{*}(\omega_1-\Omega)\varepsilon_{\mathrm{p}}(\omega_1). \quad (4)$$

Since $A(\Omega)$ is the convolution of $\varepsilon_{\mathrm{S}}(\omega)$ and $\varepsilon_{\mathrm{p}}(\omega)$, the second-order polarization of the stimulated Raman excitation is given by the product of the real electric fields of pump and Stokes pulses in time-domain:

$$\tilde{A}(t) = \mathcal{F}^{-1}(A(\Omega)) = \tilde{\varepsilon}_{\mathrm{S}}(t)\tilde{\varepsilon}_{\mathrm{p}}(t), \quad (5)$$

where $\tilde{\varepsilon}_{\mathrm{S}}(t)$ and $\tilde{\varepsilon}_{\mathrm{p}}(t)$ are the real electric fields of the Stokes and pump pulses, respectively. Taking into account the time-delay $\Delta\tau_{\mathrm{SR}}$ between pump and Stokes pulses, the excitation of the Raman mode with the stimulated Raman frequency Ω is given by the Fourier transform of the product of the electric fields in the time-domain:

$$A(\Omega, \Delta\tau_{\mathrm{SR}}) = \mathcal{F}(\tilde{\varepsilon}_{\mathrm{p}}(t)\tilde{\varepsilon}_{\mathrm{S}}(t+\Delta\tau_{\mathrm{SR}})). \quad (6)$$

3. Experimental

A femtosecond laser system (Clark-MXR Inc., CPA-2010) in combination with two optical parametric amplifiers (OPA; Light Conversion, TOPAS) is used to create the three femtosecond pulses required for the four-wave mixing process. The output of one of the OPAs is compressed to around 80 fs with a pair of prisms and split equally into two parts to create the pump and probe pulses. The output of the other OPA is used as Stokes pulse. This pulse is spectrally phase modulated in a pulse shaper arrangement. Here, the pulse is separated into its spectral components and then collimated in a zero dispersion compressor setup. The spectral phase is modulated using a liquid-crystal display (LCD; Jenoptik, SLM-640/d) placed in the Fourier plane. The phase of the spectral components of the Stokes pulse is varied by applying suitable voltages to the individual pixels [21]. With this pulse shaper, it is also possible to realize amplitude modulation but this feature is not used for the present experiment. For CARS, a folded BoxCARS configuration is chosen, which fulfills the phase-matching condition and optimally separates the anti-Stokes signal from the lasers [22]. In the experiments discussed in the following, the unchirped pump and Stokes pulses are temporally overlapped and fixed. Relative temporal shifts due to the phase shaping are part of the control and therefore not compensated (see below). The frequency difference between the pump and Stokes pulses determines which modes are coherently excited. The probe pulse monitors this mode excitation at a variable time delay. The anti-Stokes signal thus generated is spatially separated and recorded by a monochromator equipped with a CCD camera.

Fig. 1 shows the schematic diagram of the optimal control setup used for the present experiment. The optimization experiments are controlled by an evolutionary algorithm and the optimized pulse shape is characterized using the transient-grating frequency-resolved optical gating (TG FROG) technique [23]. Here, the Stokes pulse is split into three beams of equal intensity and is brought to focus in a thin sapphire plate in the folded BoxCARS geometry. The resulting TG signal is recorded with respect to the delay of one of the beams with the help of a spectrometer equipped with a CCD. FROG traces are analyzed with the software FROG 3.0.9 procured from Femtosoft Technologies, USA.

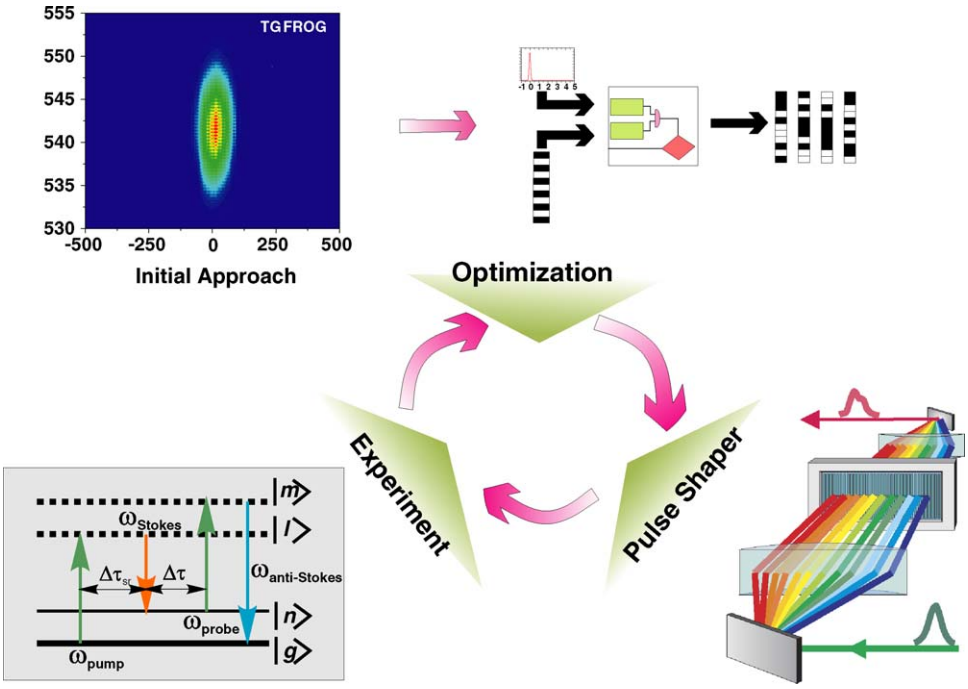

Fig. 1. Schematic description of the self-learning loop optimization. An initial guess is the starting point for the evolutionary algorithm, which controls the settings of the phase mask in a 4*f* pulse shaper. The pulse shaped by this arrangement is part of a coherent anti-Stokes Raman scattering setup. The ratio of specific Raman lines resulting from this nonlinear spectroscopy is used as fitness function for the evolutionary algorithm, which determines a new set of phase mask parameters in order to find the extremum of the fitness function.

The binary mixture of benzene and chloroform was prepared in a 50/50 v/v ratio. The liquids were purchased from Aldrich and used without further purification.

4. Results and discussion

The femtosecond CARS experiments discussed in the following were performed on a binary mixture of benzene and chloroform (henceforth called "mixture") as well as on the pure liquids. Benzene is a prototype aromatic molecule and its Raman lines are well characterized [24]. Raman active lines at 992 and 617 cm^{-1} are due to ring breathing and ring deformation modes, respectively, and lines at 849 and 1174 cm^{-1} arise from CH deformation. Chloroform is miscible with benzene and its Raman lines are well separated and less intense as compared to benzene lines. Raman lines of chloroform at 760 and 670 cm^{-1} are due to Cl–C–Cl stretching vibrations [24]. It must be mentioned that the line of benzene at 992 cm^{-1} is 10 times more intense than that of chloroform at 670 cm^{-1}. Both lines dominate the nonlinear Raman spectrum of the mixture. The optimal control tries to focus the excitation into the Raman modes of benzene and at the same time to suppress the lines of chloroform and vice versa. For the Raman excitation, a frequency difference of 800 cm^{-1} between the pump and the Stokes lasers is used. As described earlier, due to the broad spectral bandwidth of the femtosecond laser pulses (FWHM ≈200 cm^{-1}), several vibrational modes of benzene and chloroform are excited simultaneously. We would like to emphasize again that no electronic resonance is involved in this CARS process since electronic transitions for these two molecules are in the UV spectral region.

The CARS signal consists of two components: (i) a nonresonant background due to the instantaneous electronic response of the molecule (Eq. (2)) and (ii) a resonant Raman contribution (Eq. (3)). The nonresonant signal lasts for the cross correlation time of pump and Stokes pulses. To avoid the nonresonant background and artifacts arising due to zero time delay, optimizations are performed at 500 fs delay between stimulated Raman excitation and probe pulse. Before the optimization, the pump and Stokes pulses are temporally overlapped and fixed.

For all experiments discussed in the following, we employed pump and probe laser pulses of approximately 80 fs lengths. While these pulses were kept nearly transform limited during all experiments, the Stokes laser was characterized by chirp, which was varied by the optimization procedure. For the first experiment, the OPA generating the Stokes pulse was tuned to a somewhat reduced spectral width. The left side of Fig. 2A shows the CARS spectrum recorded in a mixture with the resulting nearly transform-limited Stokes pulse having a temporal width of approximately 130 fs (see FROG trace displayed in the right panel). The spectrum shows lines that can be assigned to both molecular species present in the mixture. Two intense spectral bands at approximately 992 and 670 cm^{-1} dominate the CARS spectrum. As mentioned above, the line at 992 cm^{-1} arises from benzene while the line at 670 cm^{-1} belongs to chloroform. Both lines have approximately equal intensities. Apart from these two bands, several other Raman lines contribute to the CARS spectrum but they are very weak in intensity and will not be considered in the following.

Now, we focus on exciting one molecule at a time and suppress the contribution from the other molecule present in the

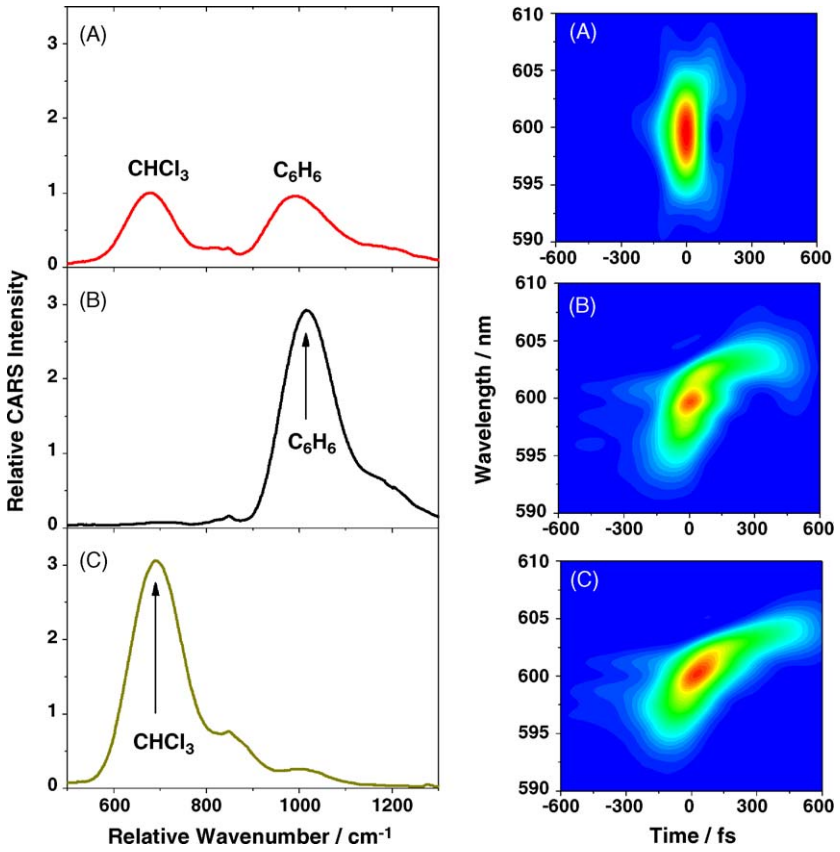

Fig. 2. Femtosecond CARS spectra taken of the mixture benzene/chloroform (left panels) and FROG traces of the Stokes laser pulses applied (right panels): (A) without optimization, (B) optimized for the benzene contribution, and (C) optimized for the chloroform line. The Stokes pulse applied for (A) had a temporal width of ≈130 fs. For the optimization a temporal shift of the Stokes pulse was admitted.

mixture. A practical consideration in a successful optimization experiment is the appropriate selection of a feedback function on which the optimization algorithm strongly depends. In our experiments, the ratio of different Raman lines observed in the CARS spectrum serves as fitness function for the evolutionary algorithm. The optimization process then results in settings for the LCD mask, which shape the Stokes pulse such that the signature of one molecule is relatively enhanced and the contribution from the other molecule is suppressed. We would like to point out that only ratios of line intensities are optimized and not absolute intensities. Nevertheless, absolute intensities will also be considered in the following discussions. The algorithm is restricted to a search of the phase function without changing the power spectrum of the Stokes pulse by amplitude modulation. For simplicity, we selected a polynomial representation of the phase function as described below [14]:

$$\phi_n = \sum_{k=2}^{K} C_k \left(\frac{n - N_0}{N} \right)^k, \quad n = 0, 1, 2, \ldots, N-1,$$

$$N = 640. \tag{7}$$

In this function of order K, the quadratic terms represent the lowest polynomial order (the linear term would result in an exclusive temporal shift of the pulse). The parameter N_0 is the offset of the phase function. A linear phase shift can be performed with this parameter. N_0 also results in a temporal shift of the pulse, which has to be taken into account when calculating the resulting overlap between pump and Stokes laser pulses. The algorithm optimizes N_0 and C_k such that Raman lines of one molecule are excited selectively in a mixture. In each optimization, 64 individuals were tested in each generation. The mutation probability was set to 0.1. The learning algorithm was able to find the optimum values after typically 15 generations. The details of this algorithm and also the influence of parameters on optimization process are described in Ref. [9].

Panel B of Fig. 2 shows the optimization result for the Raman lines of benzene and the FROG trace of the Stokes pulse resulting in the optimized spectrum. It is evident from the spectrum that the contribution from chloroform is nearly completely suppressed. The absolute intensity of the benzene line was increased by approximately 200%. The corresponding set of values are listed in Table 1. The panel C of Fig. 2 represents the optimized

Table 1
Parameters defining the settings of the LCD phase mask shaping the Stokes laser pulse for the CARS spectra displayed in Fig. 2

Measurement	Offset N_0	C_2	C_3	$\Delta\tau_{SR}$ (fs)
A	320	−411	500	0
B	132	−83	813	570
C	376	584	−1422	−110

The relative temporal shift of the Stokes laser pulse relative to the pump laser pulse ($\Delta\tau_{SR}$) is given in the last column.

CARS spectrum for the Raman lines of chloroform and the corresponding FROG trace of the Stokes laser pulse. In this case, the Raman lines of chloroform are clearly enhanced over the Raman lines of benzene. Also here an absolute enhancement of approximately 200% can be observed. The parameters obtained in this case are also given in Table 1. The experiments are repeated many times with only three parameters N_0, C_2 and C_3. In all the cases we obtained a similar set of parameters. We also have used polynomial functions of higher orders but increasing the number of parameters did not give considerably better results. This points to the fact that even simple phase structures are sufficient for spectrum control. Based on the experimental results, we observed that the three parameters are necessary and sufficient for the optimization if also N_0 is used as free parameter. Furthermore, we found that the parameters are not independently influencing the spectrum. Different values of, e.g. N_0 resulted in new combinations of C_2 and C_3 for an optimized line ratio.

The spectrogram of the Stokes pulses resulting from the optimizations are recorded with the TG FROG and analyzed by the FROG software. For the TG FROG measurement we made sure that the measured shape is close to the shape of the pulse that interacted with the sample (taking into consideration the optical components used for the CARS setup). The FROG traces are shown in the right side of Fig. 2. While the CARS spectrum obtained without optimization (A) was obtained with a Stokes laser pulse, which was only showing little linear and nonlinear chirp, the Stokes pulses resulting from the optimizations (B and C) are considerably chirped both linearly and nonlinearly.

Recently, several mechanisms were demonstrated to influence the mode excitation. (i) A sequence of pulses can resonantly drive vibrations if the frequency of the pulse train is in resonance with the molecular vibration. This "impulsive stimulated Raman excitation" successfully applied by Weiner et al. [25] can be excluded as possible mechanism for our optimization experiments. (ii) The exciting results published by Silberberg and coworkers [19,26] show the important influence of the phase shape introduced to the pulse spectrum by the LCD display of the pulse shaper. These authors enhanced vibrational modes by applying rectangular [26] or step-like [19] phase shifts to both pump and Stokes pulses or to the probe pulse. A phase step at the resonance frequency utilized the off-resonant part of the spectrum to enhance the selected mode contribution. Analyzing our optimization results clearly showed changes of the phase shape. However, none of these phase structures would explain the enhancement and suppression of the Raman lines using the Silberberg model. (iii) A "trivial" mechanism was very recently demonstrated by, e.g. Hellerer et al. [27]. Here, a time delay was introduced between the two pulses exciting the vibrational modes by a stimulated Raman process. In their experiment these authors combined a transform-limited with a linearly chirped pulse. A delay between these pulses introduced a frequency shift of a stimulated Raman excitation, since the temporally overlapping spectral parts (frequency overlap) were shifted relative to each other. Since in our experiment discussed above the optimization parameter N_0 also might introduce a temporal shift of the shaped Stokes laser pulse, a contribution of this mechanism seems to be very likely.

In order to analyze the influence of the resonance shift due to possible time delay between the pump and Stokes pulses, we used both an experimental and a theoretical approach. We found that experiment and theory gave comparable results. Experimentally, the frequency overlap was investigated using a thin quartz plate instead of the sample cell for the femtosecond CARS experiment. The laser pulses responsible for the spectra given in Fig. 2 interacted with this new medium without any electronic or Raman resonance. Based on measured nonresonant CARS spectra, the excitation intensities for selected Raman modes have been calculated by taking into account different Raman line intensities. The so-obtained spectra reflect the excitation profiles expected if solely the shifted frequency overlaps would be responsible for enhancement and suppression of Raman lines. For the theoretical analysis, the electrical fields of pump and Stokes pulses gained from FROG traces were used to calculate the spectrum of the total excitation field according to the model based on Eq. (6) given in the theory part of this contribution. On the basis of the evaluated excitation distribution the Raman amplitudes of selected vibrational modes were predicted using the temporal shift between pump and Stokes pulses introduced by the optimization procedure (as determined experimentally with the quartz plate) and considering the different Raman line intensities. The intensities of the benzene and chloroform CARS lines obtained from the optimization experiments (top row) as well as the line intensities predicted by the nonresonant test experiments (middle row) and the theory (bottom row) are displayed in the bar diagrams of Fig. 3. The most intense line in the spectrum obtained without optimization (panel A of Fig. 2) was normalized and all other intensities are scaled accordingly to have comparable relative intensities. As already mentioned above, the results from the CARS experiments on quartz and the predictions from theory are comparable. While in the case of the chloroform optimization the temporal shift between Stokes and pump laser pulses ($\Delta\tau_{SR} \approx -110$ fs) seems to contribute to the observed changes, this is clearly not the case for the optimization of the benzene Raman line ($\Delta\tau_{SR} \approx +570$ fs). Here, the observed ratio between benzene and chloroform bands is approximately 40 while the predicted ratios lie between 0.7 (experiment) and 0.8 (theory). The increase factor of the benzene line intensity is found to be approximately 3. However, the quartz experiment and the theory predict a drastic decrease of the intensity. An extreme discrepancy between predictions and observed experimental results is obvious. On the other hand, the decrease of the chloroform contribution could be explained by the frequency shift due to the time delay introduced between pump and Stokes laser pulses. Even for the optimization of the chloroform line (panel C of Figs. 2 and 3), where the correct trend for the line ratios is predicted, considerable deviations occur. Firstly, no explanation of the absolute enhancement of the chloroform band can be given. Secondly, the predicted ratios between chloroform and benzene line intensities are found to be clearly smaller in the predictions by experiment and theory than in the CARS experiment performed on the mixture.

The only explanation for our observations seems to be that the trivial mechanism based on a temporal shift of the chirped laser pulse is not or only partly applicable in our case. In order

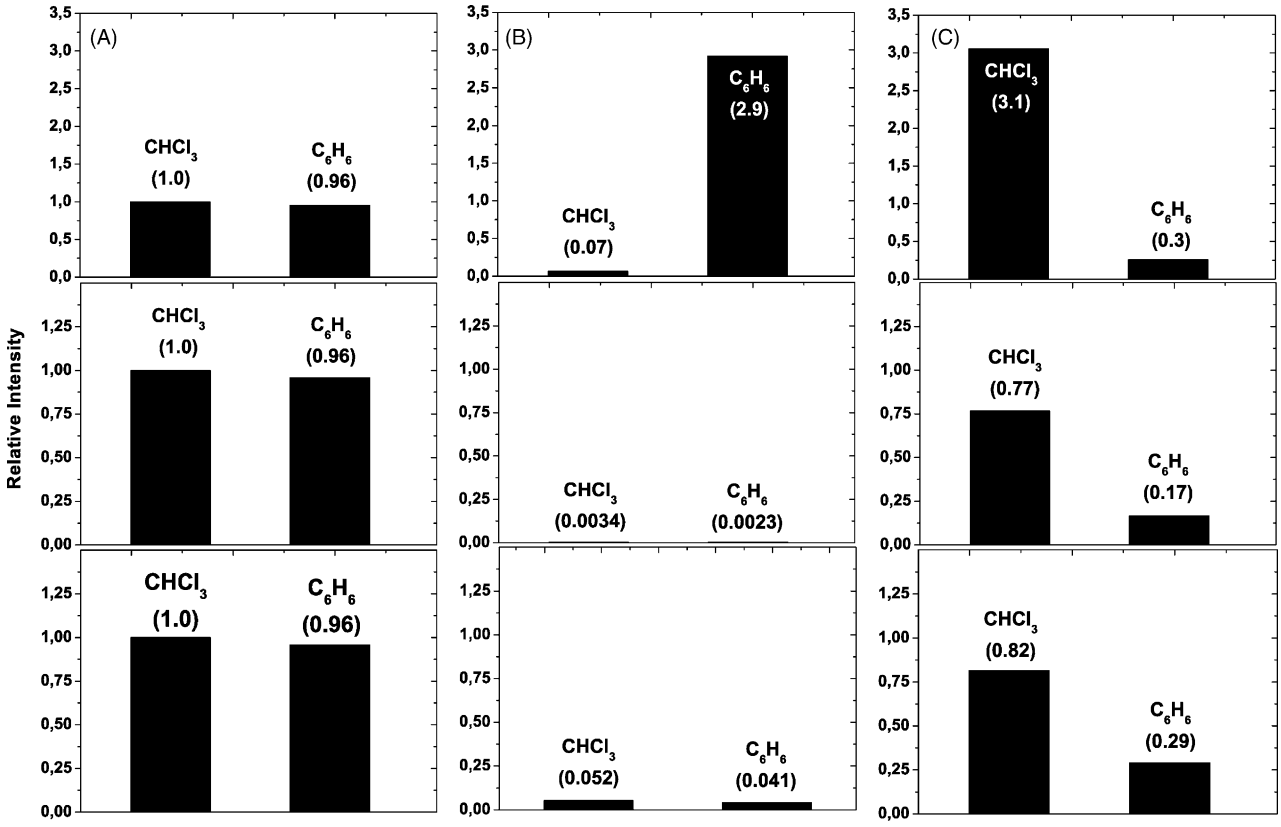

Fig. 3. Bar diagrams displaying the CARS intensities for the benzene (C_6H_6) and chloroform ($CHCl_3$) lines. (Top row) line intensities taken from the CARS signals obtained from the optimization experiments on the mixture (compare Fig. 2). (Middle row) line intensities as predicted by the nonresonant CARS measurements using a quartz plate instead of the sample. (Bottom row) line intensities as calculated using the theoretical model. The most intense line seen in the CARS spectrum taken with the transform-limited Stokes laser pulse is normalized, all other lines are scaled accordingly to have correct relative intensities.

to verify this, further experiments were performed. Two of these control experiments will be discussed in the following.

For the second experiment discussed here, the OPA generating the Stokes laser pulse was tuned to produce a broad spectrum. The compressed Stokes laser pulse now had an autocorrelation width of only ≈70 fs. Panel A of Fig. 4 gives the CARS spectrum obtained from the mixture for the unchirped laser pulses (left side) and the FROG trace of the corresponding Stokes laser pulse (right side). The reduced pulse length of the Stokes laser results in a changed intensity ratio between benzene and chloroform CARS lines as compared to Fig. 2A. Now the benzene contribution is clearly dominating the spectrum. For the optimization again parameters N_0, C_2, and C_3 were varied, admitting a temporal shift between the pump and Stokes laser pulses. The parameters for the LCD phase mask settings used to obtain the spectra displayed in Fig. 4 are listed in Table 2. Panel B shows the result of an optimization of the benzene contribution. A very effective suppression of the chloroform contribution is achieved, while the benzene line is even absolutely enhanced. In the case, where the ratio between chloroform and benzene lines was maximized to relatively enhance the chloroform contribution, the benzene contribution was nearly completely suppressed while the chloroform line was enhanced.

Since again a variation of the parameter N_0 was admitted in the optimization process, temporal shifts between Stokes and pump laser pulses occurred. The delay $\Delta\tau_{SR}$ between Stokes and pump laser pulses introduced by the optimization procedure was ≈+180 fs for the benzene and ≈−200 fs for the chloroform optimization. In the electronically nonresonant case only the temporally overlapping parts of the pump and Stokes pulses should contribute.

Taking into account the temporal width of the pulses involved, a considerable decrease of excitation intensity in the stimulated Raman process has to be expected. Again, the observed line intensities as well as the predicted ones are displayed as bar diagrams (see Fig. 5). Also in this second experiment, clear deviations from the predictions are found for the relative as well as absolute CARS intensities. In no way, an explanation by simple frequency shifts due to changes of the timing of the laser pulses is possible here. The most striking effect here and in the experiments discussed above is the absolute enhancement of lines,

Table 2
Parameters defining the settings of the LCD phase mask shaping the Stokes laser pulse for the CARS spectra displayed in Fig. 4

Measurement	N_0	C_2	C_3	$\Delta\tau_{SR}$ (fs)
A	311	−402	−23	0
B	412	−174	824	+180
C	392	657	−590	−200

The relative temporal shift of the Stokes laser pulse relative to the pump laser pulse ($\Delta\tau_{SR}$) is given in the last column.

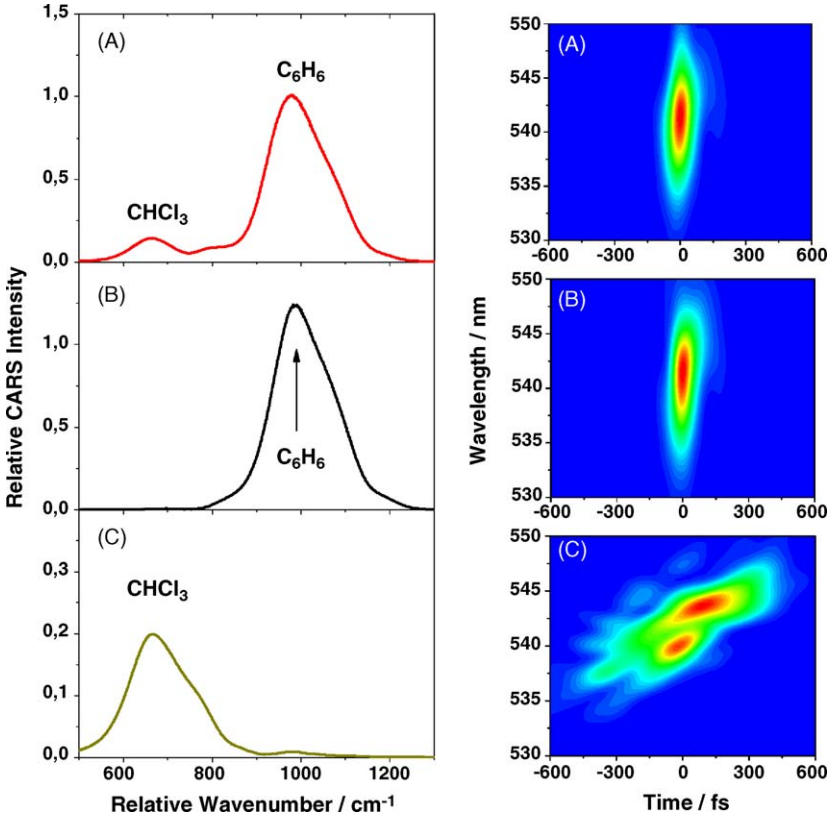

Fig. 4. Femtosecond CARS spectra taken of the mixture benzene/chloroform (left panels) and FROG traces of the Stokes laser pulses applied (right panels): (A) without optimization, (B) optimized for the benzene contribution, and (C) optimized for the chloroform line. The Stokes pulse applied for (A) had a temporal width of approximately 70 fs. For the optimization a temporal shift of the Stokes pulse was admitted.

where a considerable decrease of the CARS intensities would be predicted. It is impossible to understand this behavior based on a trivial model.

While the timing of the Stokes and pump pulses ($\Delta\tau_{SR}$) obviously does not result in an appropriate change of the Raman resonance conditions of the stimulated Raman excitation, still it has an important influence on the quality of the optimization. This can be easily verified by keeping N_0 fixed. The focussing of the excitation into one mode can be achieved not to the same degree that one achieves for free variation of N_0. The

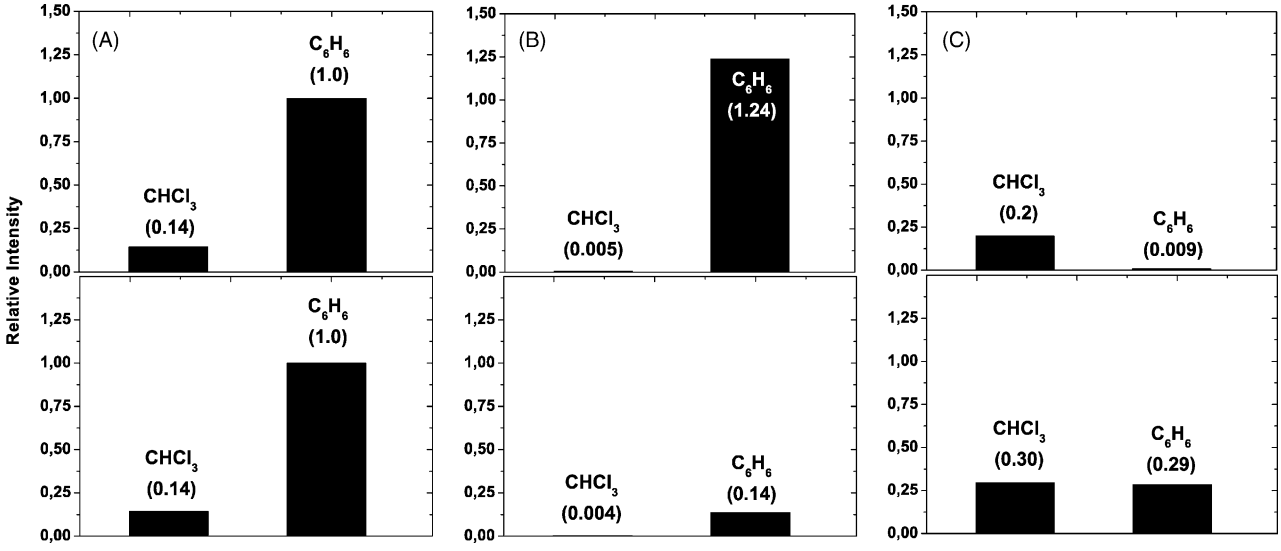

Fig. 5. Bar diagrams displaying the CARS intensities for the benzene (C_6H_6) and chloroform ($CHCl_3$) lines. (Top row) line intensities taken from the CARS signals obtained from the optimization experiments on the mixture (compare Fig. 4). (Bottom row) line intensities as calculated using the theoretical model (quartz plate experiments give comparable results). The most intense line seen in the CARS spectrum taken with the transform-limited Stokes laser pulse is normalized, all other lines are scaled accordingly to have correct relative intensities.

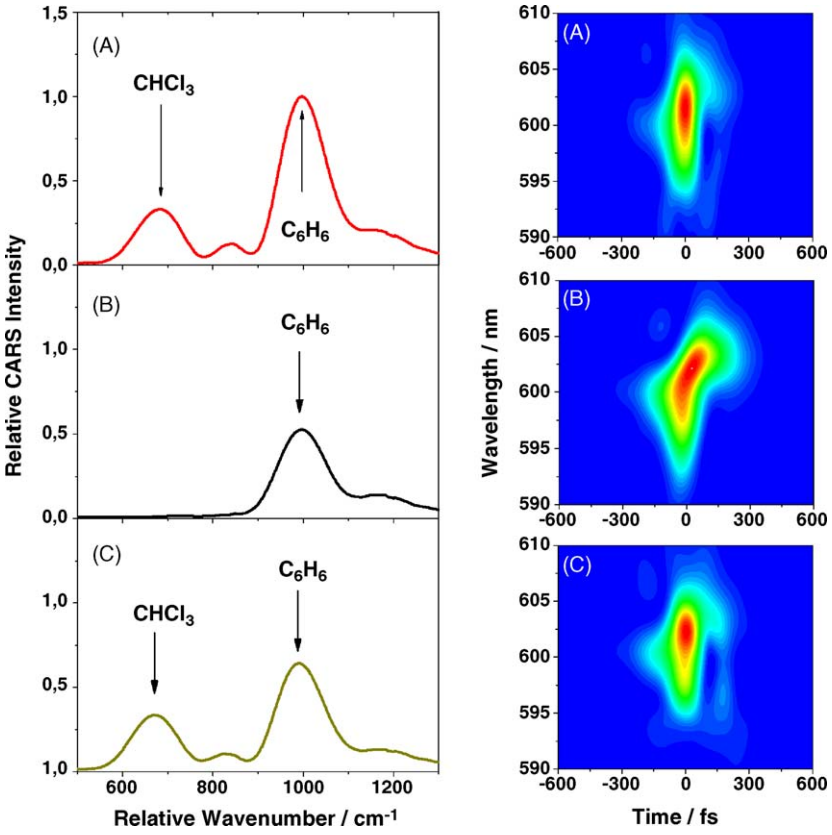

Fig. 6. Femtosecond CARS spectra taken of the mixture benzene/chloroform (left panels) and FROG traces of the Stokes laser pulses applied (right panels): (A) without optimization, (B) optimized for the benzene contribution, and (C) optimized for the chloroform line. The Stokes pulse applied for (A) had a temporal width of approximately 100 fs. For the optimization no temporal shift of the Stokes pulse was admitted.

third optimization experiment, which we will discuss here, was performed having N_0 fixed at a value resulting in $\Delta\tau_{SR} = 0$ fs. That means that no temporal shift between Stokes and pulse laser pulses was introduced by the optimization. The results of these CARS experiments are displayed in Fig. 6. Panel A again gives the CARS spectrum for the nearly transform limited Stokes pulse having a temporal width of approximately 100 fs as well as the corresponding FROG trace of this pulse. Panel B is for the benzene optimization and panel C for the optimization of the chloroform line. Here, a variation of parameters C_2–C_{10} allowed the evolutionary algorithm to take influence on the CARS line ratios. The higher order polynomial was chosen in order to give the algorithm further degrees of freedom, since without variation of N_0, the optimization proved to be less efficient (Table 3).

While the chloroform line intensity is very efficiently suppressed (see panel B), the complete suppression of the intense benzene line seems not to be possible (see panel C). The bar diagrams shown in Fig. 7 again demonstrate that the calculated spectra (or equivalently, the quartz plate experiments) cannot predict the results of the optimization experiments on the mixture. Since now a temporal shift is omitted, the frequency shifts as well as the changes of the absolute intensities are predicted to be rather small. However, the observed changes of both intensity ratios and absolute CARS intensities are considerable. In contrast to the experiments, where N_0 is varied and therefore, time delays between Stokes and pump pulses are introduced, no absolute line enhancement can be observed.

Using the data of the second experiment discussed above (see Figs. 4 and 5 and Table 2), further aspects will be considered in the following. Since in our experiments a mixture of two different molecules is investigated, the question arises, whether either a direct interaction of the molecules or a superposition of signal fields from both molecule are contributing to the observed CARS signal. For this purpose, the laser pulses used

Table 3
Parameters defining the settings of the LCD phase mask shaping the Stokes laser pulse for the CARS spectra displayed in Fig. 6

Measurement	Offset N_0	C_2	C_3	C_4	C_5	C_6	C_7	C_8	C_9	C_{10}
A	320	−411	500	0	0	0	0	0	0	0
B	320	−154	1747	−1572	122	1853	−402	625	−1393	−1072
C	320	−397	−1960	1584	−745	−1479	733	−1346	1353	1486

The relative temporal shift of the Stokes laser pulse relative to the pump laser pulse ($\Delta\tau_{SR}$) is in all cases approximately 0 fs. The parameter N_0 was kept fixed during optimization.

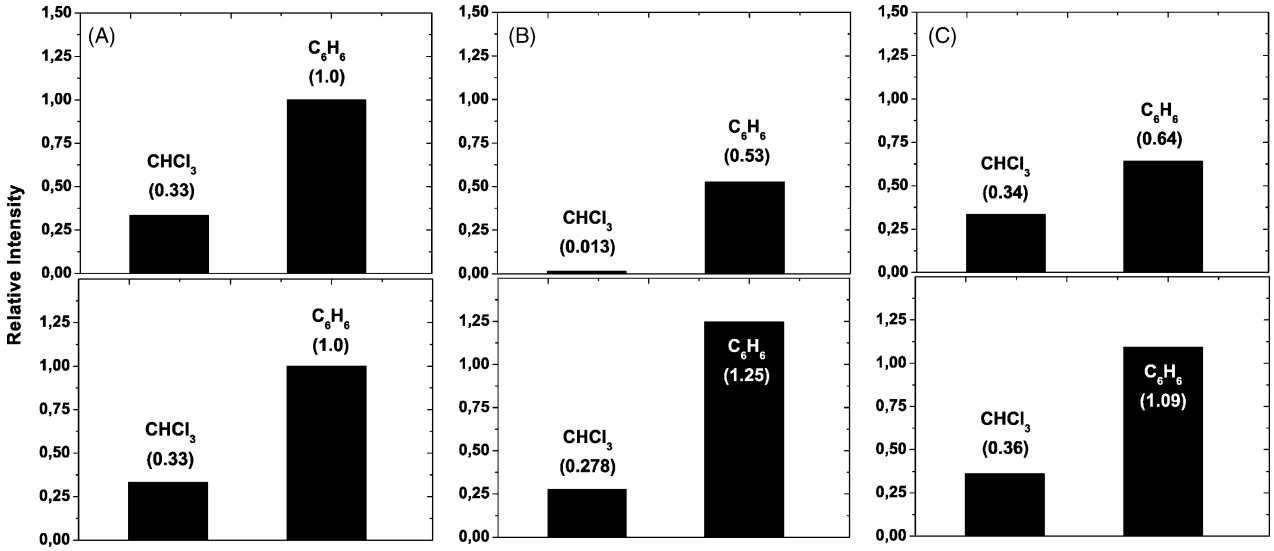

Fig. 7. Bar diagrams displaying the CARS intensities for the benzene (C_6H_6) and chloroform ($CHCl_3$) lines. (Top row) line intensities taken from the CARS signals obtained from the optimization experiments on the mixture (compare Fig. 4). (Bottom row) line intensities as calculated using the theoretical model (quartz plate experiments give comparable results). The most intense line seen in the CARS spectrum taken with the transform-limited Stokes laser pulse is normalized, all other lines are scaled accordingly to have correct relative intensities.

for the CARS experiments on the mixture were applied to the pure liquids (benzene and chloroform). No further optimization was performed. The LCD phase mask settings given in Table 2 therefore were left unchanged. Fig. 8 displays the CARS spectra obtained from pure benzene (panels A and B) and from pure chloroform (panels C and D). The upper panels show the results of CARS experiments using the optimized Stokes pulses for the respective substances (benzene: panel A; chloroform: panel C). For the spectra given in the lower panels, the Stokes pulse was optimized for the respective other molecule (chloroform: panel B; benzene: panel D). The intensity of the benzene CARS line displayed in panel A was set to unity, the other spectra are scaled accordingly to give the correct relative intensities. It becomes obvious (compare scales of panels A and C with those of panels B and D) that the suppression of line contributions works perfectly also in the pure liquid. We consider a comparison of the absolute intensities of the spectra obtained from the mixture and the pure liquids to be problematic. Therefore,

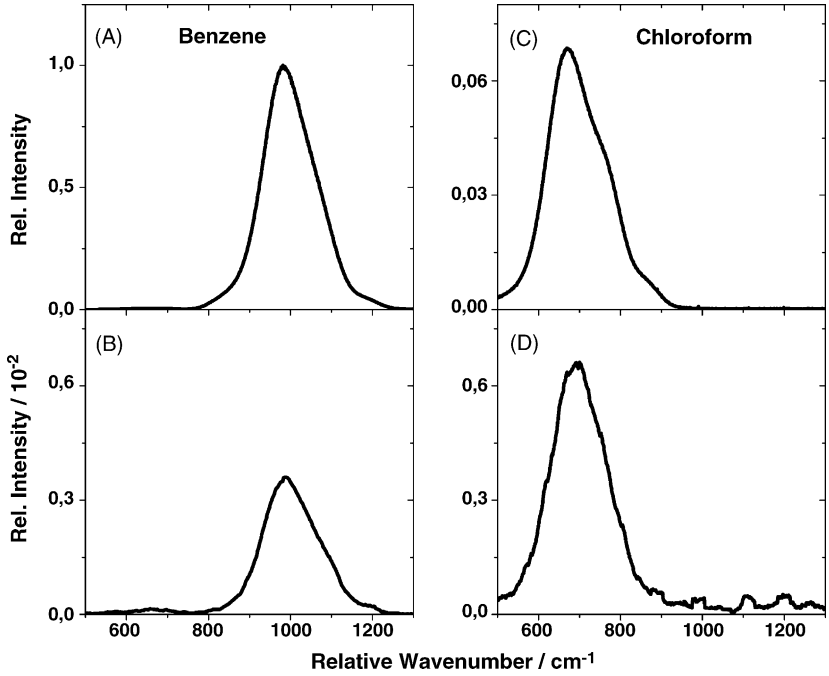

Fig. 8. Femtosecond CARS spectra taken of pure benzene (left panels) and chloroform (right panels) using the same experimental conditions as for the spectra displayed in Fig. 4 (LCD settings, see Table 2): (A) and (D) optimized for benzene (parameters of row B of Table 2), (B) and (C) optimized for chloroform (parameters of row C of Table 2). The benzene line intensity of the spectrum displayed in panel A was normalized, the other spectra are scaled to give the correct relative intensities.

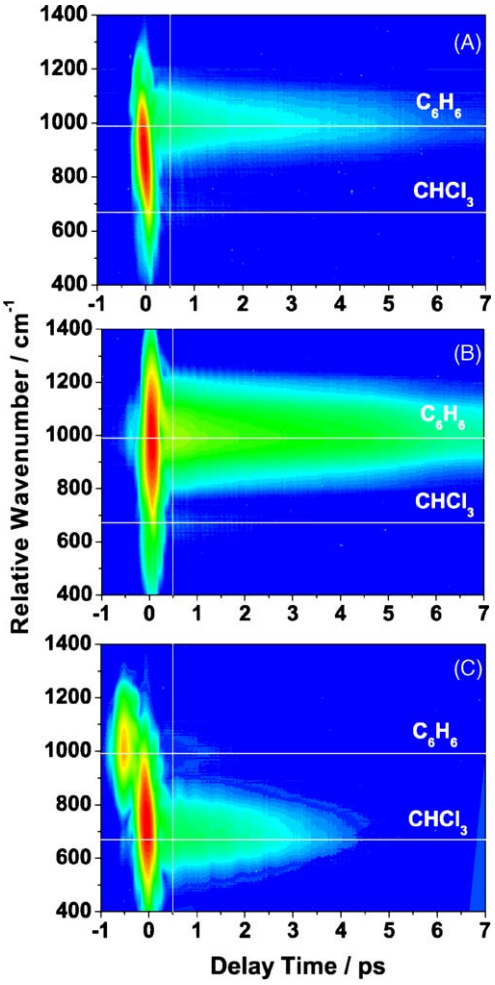

Fig. 9. CARS spectra as a function of probe delay time taken of the mixture using the same experimental conditions as for the spectra displayed in Fig. 4 (LCD settings, see Table 2): (A) for the unchirped Stokes laser pulse, (B) for the Stokes pulse optimized for the benzene signal, and (C) for the chloroform optimization. For the color-coded intensities a logarithmic scale was used.

we will not discuss this aspect here. From the experiments on benzene and chloroform the conclusion can be drawn that the optimization mechanism works on a molecular level. The spectrum control addresses specific molecules even in a mixture of different molecules.

Transient CARS signals as a function of the probe delay time were also taken in order to see whether the mode focussing is a temporally localized effect or persists for a longer time. In all cases (mixture and pure liquids) the suppression or enhancement of the CARS lines were found over the full coherence lifetime. As an example, we again use the experimental conditions as described for the second experiment. The transients are shown in Fig. 9. The dynamics observed for the transform-limited Stokes pulse is displayed in panel A, while panels B and C give the results obtained with Stokes pulses optimized for benzene and chloroform, respectively (compare Fig. 4). For the intensities a logarithmic presentation was used in order to compensate for the intense signal at $\Delta\tau = 0$. The wavenumber positions of the benzene 992 cm^{-1} and the chloroform 670 cm^{-1} lines are indicated in the transients.

The figure demonstrates the selective excitation of the molecular modes in a mixture. It is evident from panel B that in case of an optimization of the benzene lines, only the temporal behavior of the benzene modes can be observed over the full signal lifetime. The strongest line of benzene at 992 cm^{-1} dominates the transient. However, other weak modes are also present. In the transient recorded with the optimization parameters resulting from the optimization of the chloroform lines, the strong signal of benzene is suppressed. Only chloroform modes are visible and the spectrally resolved transient does not show contributions of benzene modes over the whole coherence lifetime. The peak at the spectral position of the benzene 992 cm^{-1} line that can be seen in the transient for negative delay times is due to a temporal double structure of the shaped Stokes pulse (compare FROG trace shown in Fig. 4C). At this position the probe pulse interacts with the Stokes pulse and the pump laser acts as probe at a fixed delay time. Interestingly, for the new time-ordering, the optimization of the Stokes pulse for chloroform lines enhancement is not valid anymore.

We have also considered the effect of nonlinear propagation effects inside the liquid sample in order to rule out the observed enhancement of vibrational modes due to pulse shaping. It is likely that the learning algorithm is simply compensating for nonlinear propagation effects in the liquid, rather than exciting the molecule. Care has been taken to minimize this effect. The liquid sample was contained in a 1 mm path length cuvette. In order to rule out unwanted nonlinear effects, we have checked for white light generation by measuring the pulse spectra before and after the sample cell. The observation that the pulses optimized for a particular Raman mode in a mixture also works well with the individual substances, also supports our assumption that such effects do not contribute to the observed spectra.

5. Summary and conclusions

We have discussed results obtained from femtosecond time-resolved coherent anti-Stokes Raman scattering (CARS) spectroscopy performed on a mixture of benzene and chloroform. In order to suppress or enhance Raman lines in the nonlinear spectrum, we have applied a self-learning loop approach for optimal control. The shape of the Stokes laser pulse was changed by means of a phase only modulation in a 4*f* pulse shaper arrangement with a computer-controlled LCD phase mask. A polynomial function is used in order to simplify the programming of the phase mask. If a temporal shift between pump and Stokes laser pulses is allowed during the optimization by the evolutionary algorithm, with only three free parameters for different experimental starting conditions a dramatic change of the CARS spectrum is achieved. A molecule-specific suppression and (relative and absolute) enhancement of the CARS lines is achieved. Leaving the time delay between pump and Stokes laser pulses fixed at, e.g. 0 fs, even a greater number of free parameters does neither result in a complete suppression of strong lines nor does it absolutely enhance line intensities. Nevertheless also here considerable changes are observed. In order to gain a better understanding of the mechanism responsible for the spectral changes, we have used the measured pulse shapes to calculate

the expected spectra and additionally checked this result by taking the spectrum from a quartz plate. It could be shown that a frequency shift due to a change of the pump–Stokes overlap (e.g. caused by a time delay between the unchirped pump and the chirped Stokes laser pulses) did not at all explain the observed spectral changes in the mixture CARS spectra. Especially the absolute enhancements of the nonlinear Raman lines are completely contrary to the predictions. Furthermore, experiments on pure liquids (benzene or chloroform) using the pulses obtained from the optimizations of the mixture spectra were performed. These demonstrated that no interaction between the molecules or superposition of the nonlinear signals of both species are required to achieve efficient suppression of bands in the CARS spectra. Transient CARS spectra taken as a function of the probe laser delay showed that the mode focussing persists for the whole lifetime of the CARS signal.

A closer investigation of the experimental results rules out all simple explanations for the mode control. Especially trivial variations of the frequency overlap of pump and Stokes laser pulses resulting in adapted stimulated Raman excitation at best are small contributions to the line suppression and enhancement mechanism. Neither pulse sequences nor step-like phase modulations are observed. Since for the CARS interaction no electronic resonances are involved, only the ground state dynamics can be made responsible for the control effect. At the moment, experiments on different molecular systems also using a variation of the spectral amplitudes within the pulse shaper setup are performed. Further insight into the control mechanism should be possible with data from these measurements.

Variation of the experimental conditions (e.g. lengths of the laser pulses) have a strong influence on the spectra. Nevertheless, the feedback-controlled optimization always yields comparable results, which is a useful aspect for possible applications. The technique of spectrum control might be of interest for mode-selective investigations of ultrafast molecular dynamics. The selection of spectral lines can create favorable contrasts, which can be used for the microscopic investigation of complex structures.

Acknowledgements

We are very grateful to Drs. Dirk Zeidler and Torsten Balster (IUB) for their support in writing parts of the software. Many thanks to Abraham Scaria (IUB) for his continuous help in the laboratory. Spontaneous Raman spectra were provided by Malte Sackmann (IUB). Fruitful discussions about theoretical aspects of this work with PD Dr. Ulrich Kleinekathöfer (Univ. Chemnitz) are highly acknowledged. We thank the German Science Foundation DFG (Grant No. MA 1569/10–1) for financial support of this project.

References

[1] A.H. Zewail, Femtochemistry: Ultrafast Dynamics of the Chemical Bond, vol. I+II, World Scientific, Singapore, 1994.
[2] J. Manz, L. Wöste (Eds.), Femtosecond Chemistry, VCH, Weinheim, 1995.
[3] A. Materny, T. Chen, M. Schmitt, T. Siebert, A. Vierheilig, V. Engel, W. Kiefer, Appl. Phys. B 71 (2000) 299.
[4] T. Chen, A. Vierheilig, P. Waltner, M. Heid, W. Kiefer, A. Materny, Chem. Phys. Lett. 326 (2000) 375.
[5] D.J. Tannor, R. Kosloff, S.A. Rice, J. Chem. Phys. 85 (1986) 5805.
[6] A.P. Peirce, M. Dahleh, H. Rabitz, Phys. Rev. A 37 (1988) 4950.
[7] R. Kosloff, S.A. Rice, P. Gaspard, S. Tersigni, D.J. Tannor, Chem. Phys. 139 (1989) 201.
[8] R.S. Judson, H. Rabitz, Phys. Rev. Lett. 68 (1992) 1500.
[9] D. Zeidler, S. Frey, K.L. Kompa, M. Motzkus, Phys. Rev. A 64 (2001) 023420.
[10] C.J. Bardeen, V.V. Yakovlev, K.R. Wilson, S.D. Carpenter, P.M. Weber, W.S. Warren, Chem. Phys. Lett. 280 (1997) 151.
[11] A. Assion, T. Baumert, M. Bergt, T. Brixner, B. Kiefer, V. Seyfried, M. Strehle, G. Gerber, Science 282 (1998) 919.
[12] T.C. Weinacht, J. Ahn, P.H. Bucksbaum, Nature 397 (1999) 233.
[13] J.L. Herek, W. Wohlleben, R.J. Gogdell, D. Zeidler, M. Motzkus, Nature 417 (2002) 533.
[14] D. Zeidler, S. Frey, W. Wohlleben, M. Motzkus, F. Busch, T. Chen, W. Kiefer, A. Materny, J. Chem. Phys. 116 (2002) 5231.
[15] T. Kobayashi, M. Yoshizama, U. Stamm, M. Taiji, M. Hasegawa, J. Opt. Soc. Am. 7 (1990) 1558.
[16] T. Chen, A. Vierheilig, P. Waltner, W. Kiefer, A. Materny, Chem. Phys. Lett. 325 (2000) 176.
[17] J. Konradi, A.K. Singh, A. Materny, Phys. Chem. Chem. Phys. 7 (2005) 3574.
[18] S. Mukamel, Principles of Nonlinear Optical Spectroscopy, Oxford University Press, Oxford, 1995.
[19] D. Oron, N. Dudovich, D. Yelin, Y. Silberberg, Phys. Rev. Lett. 88 (2002) 063004.
[20] T. Polack, D. Oron, Y. Silberberg, Chem. Phys. 318 (2005) 163.
[21] A.M. Weiner, Prog. Quantum Electron. 19 (1995) 161.
[22] A.C. Eckbreth, Appl. Phys. Lett. 32 (1978) 421.
[23] R. Trebino, K.W. DeLong, D.N. Fittinghoff, J.N. Sweetser, M.A. Krummbügel, B.A. Richman, Rev. Sci. Instrum. 68 (1997) 3277.
[24] F.R. Dollish, W.G. Fateley, F.F. Bentley, Characteristic Raman Frequencies of Organic Compounds, Wiley, New York, 1974.
[25] A.M. Weiner, D.E. Leaird, G.P. Wiederrecht, K.A. Nelson, Science 247 (1990) 1317.
[26] D. Oron, N. Dudovich, D. Yelin, Y. Silberberg, Phys. Rev. A 65 (2002) 43408.
[27] T. Hellerer, A.M.K. Enejder, A. Zumbusch, Appl. Phys. Lett. 85 (2004) 25.